13th International Brick and
Block Masonry Conference
Amsterdam, July 4-7, 2004

RAIN PENETRATION THROUGH THIN LAYER MORTAR BRICK FACADES WITH OPEN VERTICAL JOINTS

Janssen H.[1]*, W. Desadeleer[1], B. Blocken[1] and J. Carmeliet[1,2]

Abstract

Thin layer mortar brick facades are generally constructed with open vertical joints, which may increase the rain penetration risk. The study focuses on the frequency and intensity of runoff on ceramic brick facades, as a continuous water film over the open joints forms a premise for rain penetration through open joints. Combined CFD and HAM modeling reveals that large parts of the ceramic brick facades can adequately buffer all impinging driving rain: runoff will only arise occasionally at the upper edge. This low intensity runoff will however not yield a water film over the vertical joints: substantial rain penetration can therefore be considered improbable for ceramic brick facades.

Key Words

Driving rain, runoff, rain penetration, thin layer mortar brick facade

1 Introduction

Thin layer mortar masonry forms a promising new building technique for brickwork, since it yields improved mechanical properties, widens the available esthetical possibilities and enables the prefabrication of brickwork units. For ease of construction, thin layer mortar masonry is commonly carried out with open vertical joints. Those open vertical joints do however sacrifice the rain tightness of the outer leaf, and may hence increase the risk on rain penetration through the facade. Rain penetration may affect the insulating quality of the envelope, cause mould forming or rotting processes or lead to a decreased durability of the facade, and should thus be carefully studied.

Rain penetration through open vertical joints can stem from directly impinging rain drops, or from a water film on the exterior surface, draining to the interior of the outer leaf under wind pressures, gravity or capillary forces. Direct impinging of rain drops is improbable, as the geometry of the vertical joints dictates a narrow window for

[1] Laboratory of Building Physics, Department of Civil Engineering, Catholic University of Leuven, Kasteelpark Arenberg 51, 3000 Leuven, Belgium.
[2] Building Physics Group, Faculty of Building and Architecture, T.U.Eindhoven, P.O. box 513, 5600 MB Eindhoven, The Netherlands.
* Corresponding author: hans.janssen@bwk.kuleuven.ac.be.

potentially threatening wind directions. The geometry similarly necessitates relatively high wind speeds, which are unlikely in combination with significant precipitation (Sneyers et al, 1979).
The presence of a continuous water film on the exterior surface thus forms a premise for potential rain penetration through open vertical joints in thin layer mortar masonry. The risk on rain penetration is consequently determined by the frequency and the intensity of moisture runoff on thin layer masonry facades. In this paper, the frequency and intensity of moisture runoff is analyzed with a Computational Fluid Dynamics (CFD) based model for driving rain and a Heat and Moisture transport (HAM) model for moisture absorption and storage in capillary active materials.

2 Building typologies

In this paper, the frequency and intensity of moisture runoff are analyzed for the facades of four basic types of stand-alone buildings (Figure1). Type 'a' is a high building, while type 'b' is a long and moderately high building. In type 'c' a vertical opening is situated in the middle of a long and moderately high building. Type 'd' is similar to type 'a', but adds an underpass. Types 'c' and 'd' are included to study the effect of openings on the local intensity of driving rain.

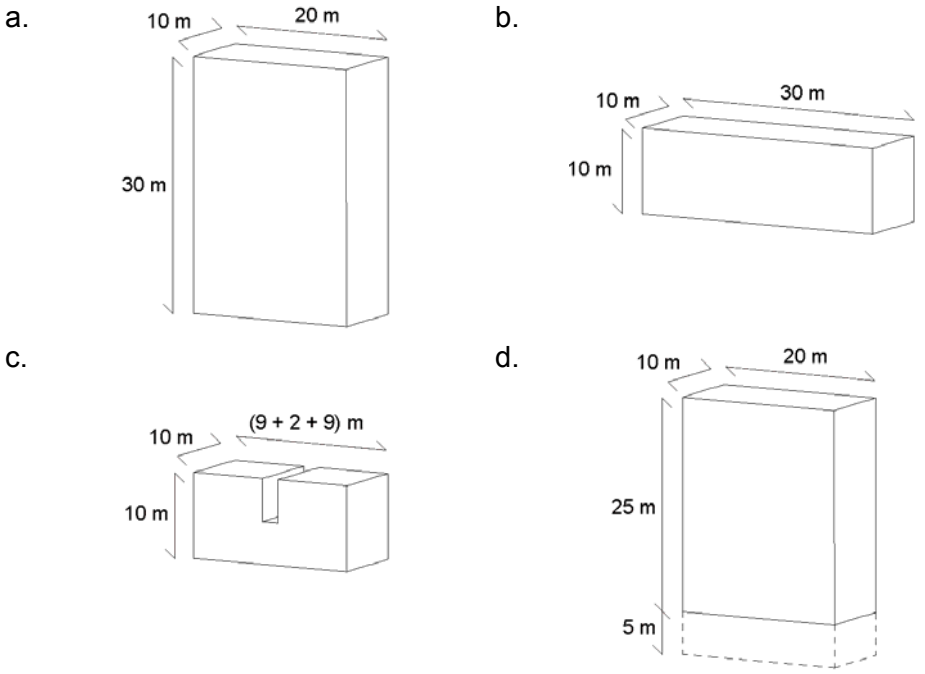

Figure 1: Building typologies analyzed in this paper: (a) tall building, (b) low long building, (c) low long building with central opening, (d) tall building with underpass.

3 Driving rain intensities

For the calculation of the driving rain intensity on the building facades, the methodology as developed by Blocken and Carmeliet (2000a, 2000b, 2002) is employed. They relate the driving rain intensity to the reference rain intensity by means of catch ratio η, which is defined as:

$$\eta(t) = \frac{R_{dr}(t)}{R_h(t)} \quad (1)$$

$\eta(t)$ is the catch ratio (-);
$R_{dr}(t)$ is the driving rain intensity (l/m²h);

$R_h(t)$ is the reference rain intensity (l/m²h).

The calculation method for the catch ratio consists of three steps:

3.1 Steady state wind flow pattern

The steady-state wind flow pattern around the buildings is simulated applying CFD. The Reynolds Averaged Navier-Stokes equations (RANS) and continuity equation are solved using the control volume method (with commercial code Fluent 5.4). Closure is obtained by using a version of the k-ε turbulence model. Results are the numerical values for the wind speed (x,y,z-components), the pressure and the turbulence quantities at the centre of each volume. Figure 2 illustrates the wind speed vectors in the vertical plane through the middle of the buildings. Figure 2a clearly shows wind deceleration (wind blocking) by the building and the important acceleration (speed up) of the wind at the vertical upwind building edges. High wind speeds can also be noted in the opening in the building and in the underpass. These high values are caused by pressure-short-circuiting between wind (overpressure) and leeward (underpressure) side.

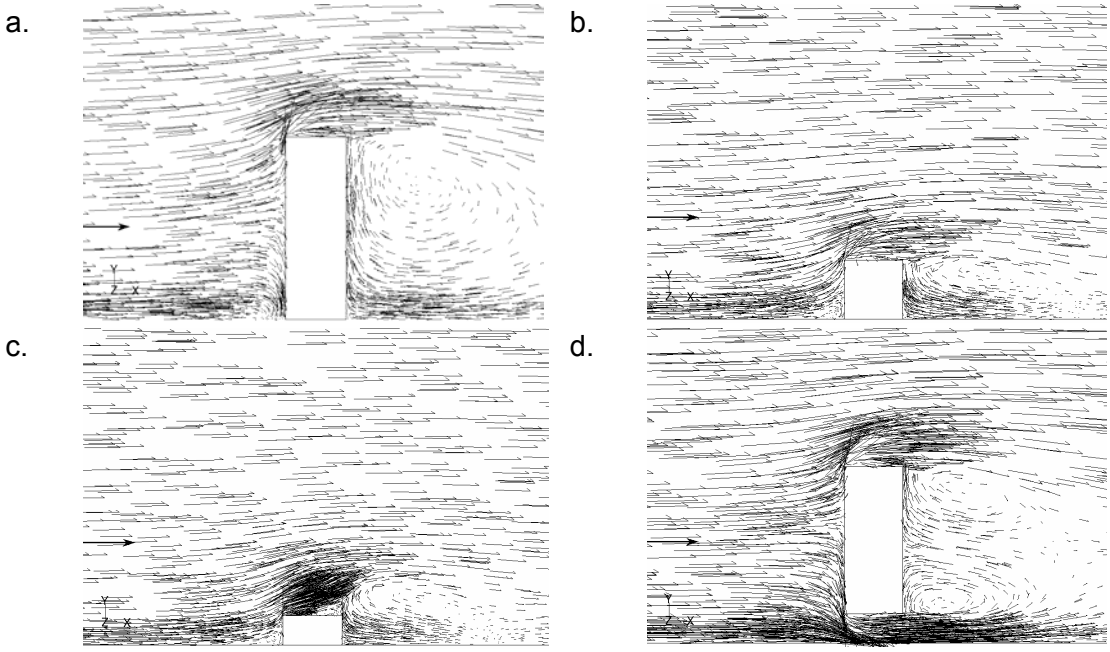

Figure 2: Wind velocity vectors in the vertical plane through the middle of the buildings. The reference wind speed at 10 m height (U_{10}) is 5 m/s.

3.2 Raindrop trajectories

With the obtained wind flow pattern, rain drop trajectories are calculated. The rain drops are injected from a horizontal plane located in the upstream-undisturbed wind flow, high above the ground: its location must allow the injected rain drops to attain the terminal fall velocity (vertical) and wind velocity (horizontal) before entering the flow pattern disturbed by the building's presence and its surroundings.

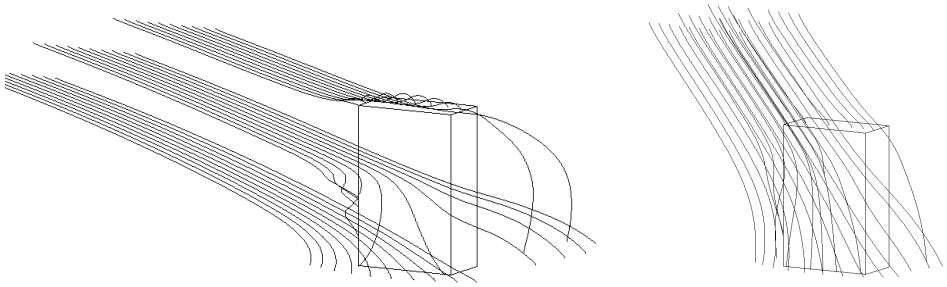

Figure 3: Perspective view of the rain drop trajectories for droplets having a diameter of 0.6 mm (left) and 2 mm (right), for building 'a' and U_{10} equal to 5 m/s.

Droplets, with diameters from 0.5 to 6 mm, are injected in the wind-flow field, with wind speeds from 0 to 10 m/s. An example is given in Figure 3. In general, it is observed that for smaller drops and at higher wind speeds, the trajectories are more inclined and their deviation near the building becomes more pronounced. For larger drops (higher inertia) and at lower wind speeds, the trajectories are less inclined and more rectilinear.

3.3 Specific and integrated catch ratio

To obtain the specific catch ratio (for one particular rain drop radius), rain drops with the given radius are released in a dense horizontal rectangular grid in the upstream wind. A large number of the released drops hit the building facade. Each three nearby rain drops in the injection plane form a triangle with area A_h. The end positions of these trajectories also form a triangle, on the building facade, with surface A_f. The specific catch ratio η_d is, according to the law of mass conservation, given by:

$$\eta_d(t) = \frac{R_{dr}(d,t)}{R_h(d,t)} = \frac{A_h(d)}{A_f(d)} \quad (3)$$

$\eta_d(t)$ is the specific catch factor (-) for rain drop radius d (m);
$R_{dr}(d,t)$ is the driving rain intensity (l/m²h) for rain drop radius d;
$R_h(d,t)$ is the reference rain intensity (l/m²h) for rain drop radius d;
$A_h(d)$ is the injection plane area (m²) for three rain drops with radius d;
$A_f(d)$ is the building facade area (m²) for three rain drops with radius d;

The integrated catch ratio η for a position on the facade is obtained by multiplying η_d for each raindrop diameter d with the fraction of these drops in the rain spell and integrating over all raindrop diameters:

$$\eta = \int_d f_h(d)\ \eta_d(d)\ \partial d \quad (4)$$

$f_h(d)$ is the raindrop size distribution through a horizontal plane (Best,1950);

This means that, for a fixed wind direction and a fixed position on the facade, wind speed and rainfall intensity unambiguously define the catch ratio. The dependency is illustrated in Figure 4, for the top corner and for the center of building type 'a'. At the top corner the catch ratio increases almost linearly with wind speed, reaching values of more than two. The highest catch ratios are observed for low rainfall intensities, which is an indication of the sweeping effect (both upwards and sideward) that is typical for small rain droplets at building corners (Blocken and Carmeliet, 2002). Catch ratios in the center of the facade are much lower, indicating its relatively 'sheltered' nature.

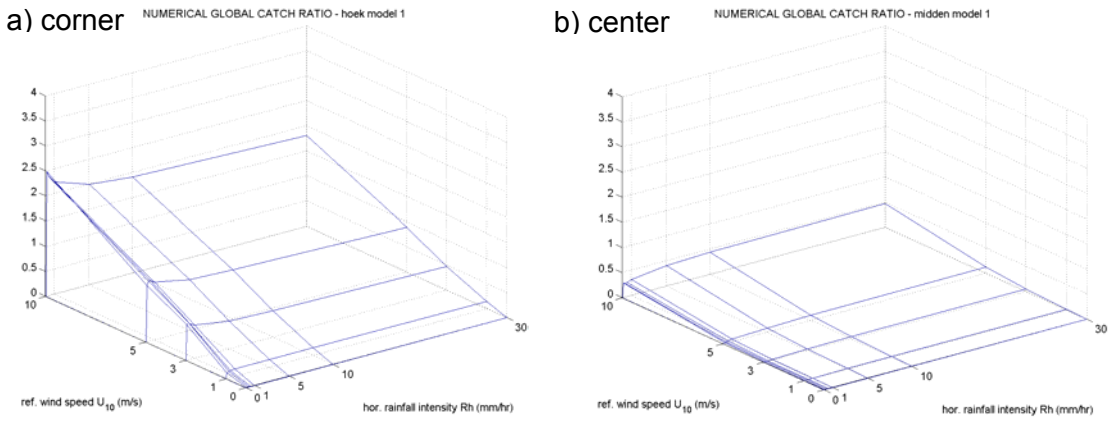

Figure 4: Catch ratio's as a function of wind speed and horizontal rainfall intensity for two positions on building type 'a'. The wind direction is perpendicular to the facade.

The distribution of the catch ratio over the facades for the different building types is given in Figure 5, for R_h equal to 5 l/m²h and U_{10} equal to 5 m/s. The figures show that driving rain intensities are much higher at the upper edge and corners for all building types. The catch ratio at the upper edge and corners increases with height of the building type. For the high rise building 'a', a completely sheltered zone exists at the bottom of the building. Such sheltered zone disappears for the lower building types (Figure 5b,c). Driving rain intensities increase locally at the opening in the building 'c' (Figure 5c), particularly at the lower edge. The higher catch ratio can be explained by the local increase in wind speed at this point (see Figure 2c). The presence of the underpass (Figure 5d) leads to a small upwards shift of the sheltered zone. We note that although locally high wind speeds are present in the underpass, this does not result in driving rain in the middle of the building. The underpass however causes the sheltered zone to shrink laterally due to higher catch ratios at the edge of the building.

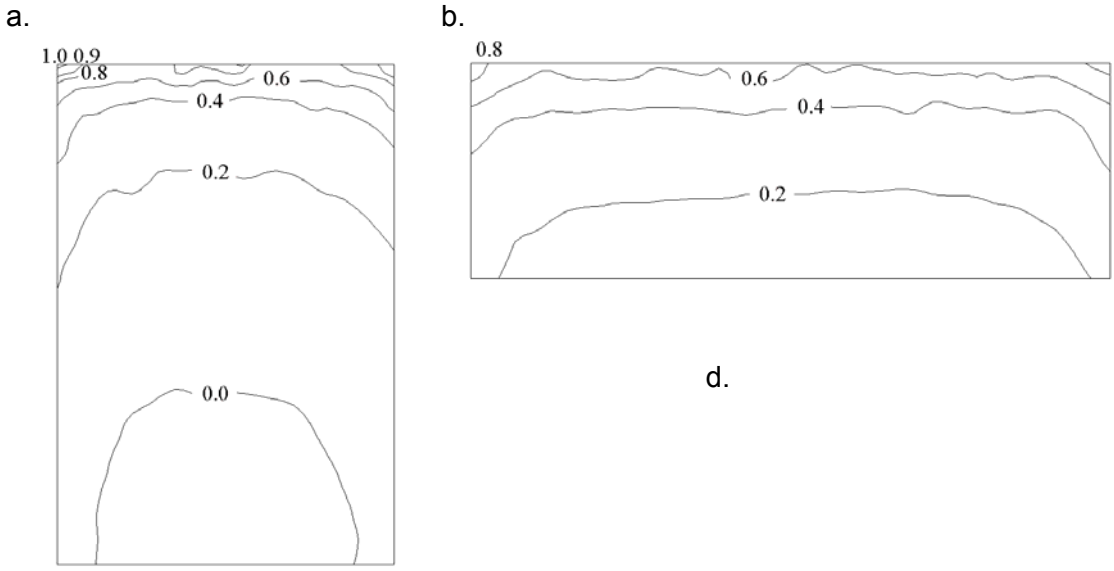

c.

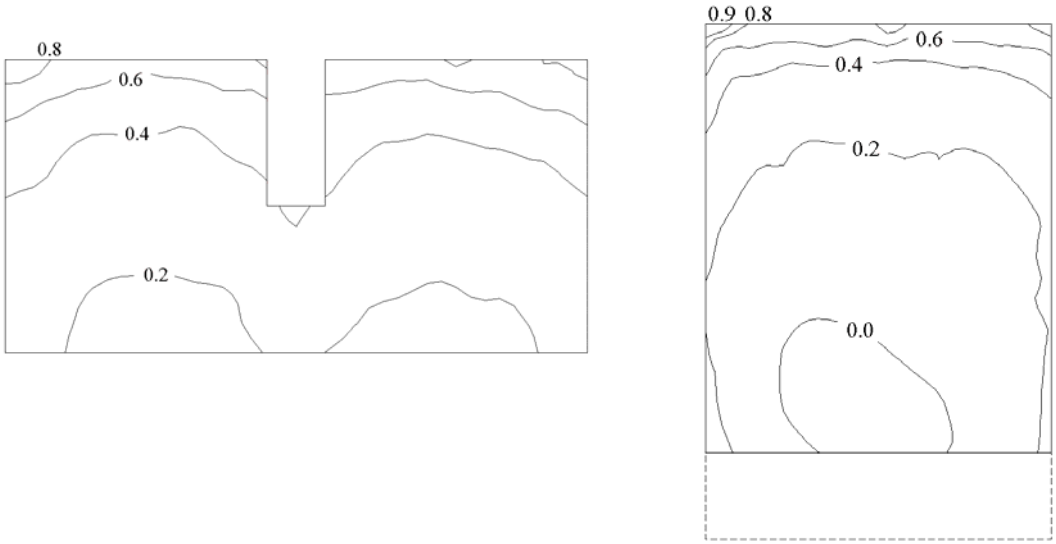

Figure 5: Contours of the catch ratio over the facade (R_h = 5 mm/h, U_{10} = 5 m/s).

4 Moisture absorption and storage

Moisture runoff on thin layer mortar masonry facades is not only governed by the driving rain supply, but equally by the storage and transport properties of the facade's outer leaf. To quantify the runoff frequency and intensity, the obtained catch ratios are implemented in a HAM simulation model.

The simulation model solving the heat and moisture transfer in a capillary active material joins the energy and mass balances, heat and moisture transfer equations, and exterior and interior boundary and climatic conditions.

In the material heat is transferred by conduction and as sensible and latent heat linked to moisture transfer in the liquid and gaseous phase. Conduction is described by Fourier's law, where the thermal conductivity depends on both moisture content and temperature. The thermal capacity is the sum of the thermal capacities of dry material and liquid water (the thermal capacity of the air-vapor mixture is neglected).

Transfer of moisture takes place in both the liquid and the gaseous phase. Darcy's law is assumed valid for the description of liquid transfer, while Fick's law is used for transfer in the gaseous phase (vapour transfer by advection is excluded). The capillary pressure is assumed to be the driving potential, directly for liquid transfer and by Kelvin's law for vapour transfer. The vapour and liquid permeabilities depend on both moisture content and temperature. Liquid moisture capacity is computed as the derivative of the moisture retention curve, for which the imbibition curve until capillary moisture content is used.

At the exterior, the heat balance consists of heat exchange by convection, net incoming radiation (short-wave direct and diffuse radiation, long wave sky irradiance and surface emission), latent heat transfer by evaporation and sensible heat transfer by driving rain. As long as the surface does not reach the capillary moisture content, transfer of moisture to and from the exterior surface is made up of evaporation and driving rain. Driving rain arriving on the facade is assumed to be entirely absorbed (no splash-off). Water vapour transfer is described with a convective surface coefficient, for which conformity between the thermal and the hygric boundary layer near the surface is assumed. During heavy rainfall or when the surface has a high initial moisture content (e.g. due to undercooling condensation), the amount of moisture supplied to the exterior surface may exceed the possible inflow into the material. The excess rainfall stacks on the surface and may run off. The runoff intensity results from the unbalance

between the supply and the inflow of moisture into the material. During runoff a fixed zero capillary pressure is maintained at the exterior surface boundary. It is assumed that runoff does not flow down the façade, but instead is discharged from the system. A model including moisture film flows on the exterior surface was presented in (Blocken et al, 2002).

The numerical solution of the one-dimensional heat and moisture transport equations is calculated using a finite-element code (Janssen, 2002). The non-linear set of equations is solved iteratively by use of the consistent Newton-Raphson scheme. To allow smaller time steps during driving rain periods and larger time steps while drying, a variable-time-step algorithm is employed in the model. The fully coupled extension (Janssen, 2002) of the mass conservative scheme of (Celia, 1990) is furthermore implemented.

5 Frequency and intensity of runoff on brick facades

The occurrence of runoff is calculated for the top corner and the center of a ceramic brick cavity wall, for the four building types. The effect of the thin mortar layer and the vertical joints on the moisture response of the wall is assumed negligible: simulations are carried out one-dimensionally.
The insulation layer and inner leaf are simplified to a constant heat transfer coefficient of 0.7 W/m²K. Since this study focuses on driving rain, all vapour transfer to the interior is omitted. The moisture retention curve and the permeabilities are obtained from standard experiments, applying the material determination methodology as proposed by Carmeliet and Roels (2001, 2002). Two different types of ceramic brick are considered, which are described by the capillary absorption coefficient A_{cap} and capillary moisture content w_{cap}, for simplicity. The latter is defined here as the moisture content when the moisture front reaches the top of a specimen in a free capillary absorption experiment, the former is a measure for the rate of water uptake (slope of the moisture mass uptake curve versus square root of time).

Brick type 'A' is characterized by a high A_{cap} (0.59 kg/m².s$^{0.5}$) and high w_{cap} (225 kg/m³), which means that this brick will easily take up driving rain and can furthermore buffer a high amount of driving rain. Brick type 'B' shows a moderate A_{cap} (0.14 kg/m².s$^{0.5}$) and a low w_{cap} (82 kg/m³), indicating a limited buffer capacity. It should be noted that A_{cap} and w_{cap} are one order of magnitude smaller for concrete bricks, which will greatly affect their absorption and buffering capacities.
In this paper, the Design Reference Year (DRY) for Essen, Germany (Grunewald, 1997) is used for the exterior climatic conditions. We are aware of the limitations of these data, as the applied selection method for the precipitation data does not necessarily reproduce the average duration of the precipitation (Künzel, 1993). Blocken and Carmeliet (2000b) moreover demonstrated that the non-weighted hourly averaging of precipitation and wind speed may distort driving rain calculations. Note ultimately that even minor variations in topography or landscape can notably influence the microclimatic wind speed and rainfall intensity close to the building. Transformation of weather station data to their meso- and microscale values, to be used in driving rain models, is still subject of (future) research. Here we assume that the inlet wind profile is consistent with the surface roughness.

Figure 6 shows time sequences of the average moisture content, the moisture content at the surface and the driving rain index ($R_h.U_{10}.\cos(\theta-\varphi)$, where θ is the wind direction and φ the façade's orientation) for the building type 'a' top corner, oriented southwest. When the surface moisture content is equal to w_{cap}, runoff occurs.

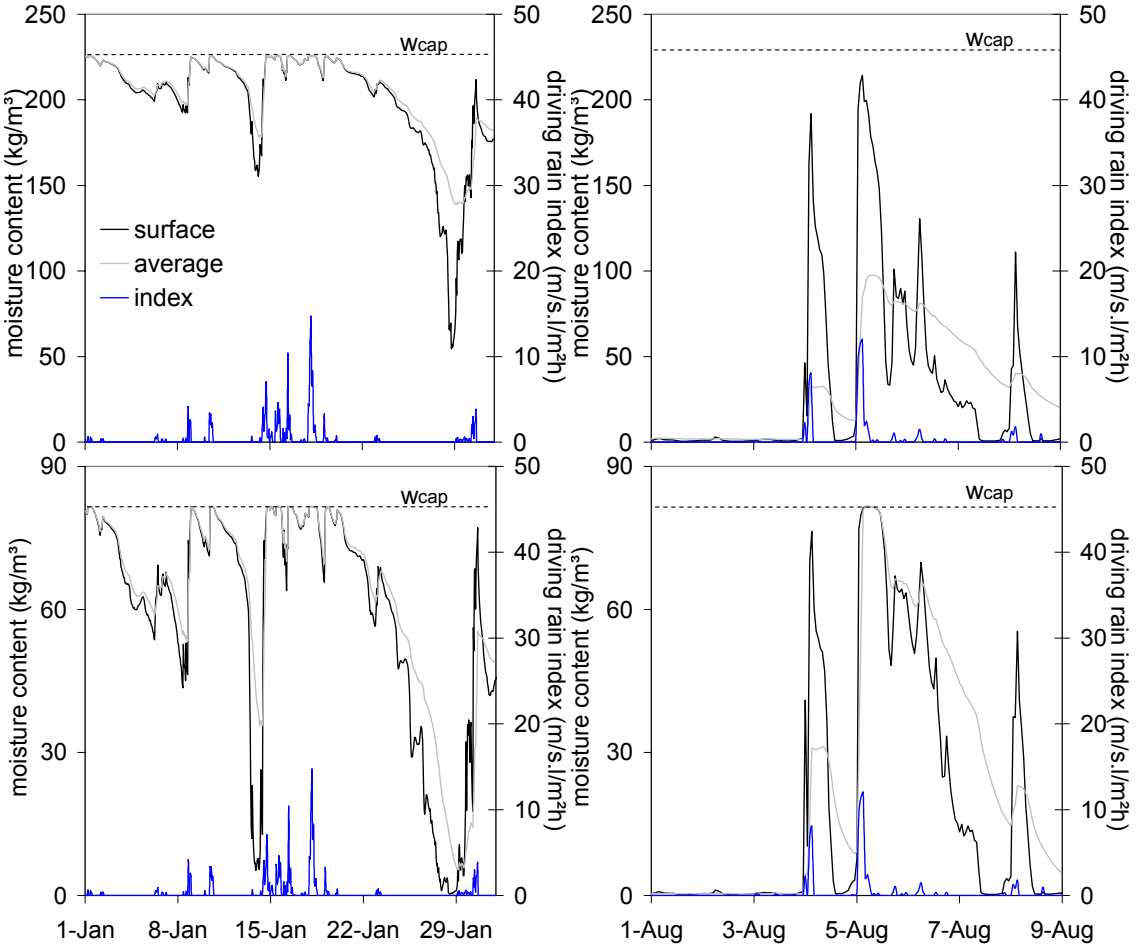

Figure 6: Time sequence of average moisture content, surface moisture content and driving rain index at the top corner of building 'a' for a southwest orientation: winter (left) and summer (right), material 'A' (top) and 'B' (bottom).

Figure 6 (left) shows the moisture response during winter for brick 'A' with high moisture buffering capacity and brick 'B' with low moisture buffering capacity. It can be noted that when runoff occurs, the average moisture content equals w_{cap} for both brick types, which indicates that runoff occurs when the brick is entirely capillary saturated. This saturation is a result from the earlier buffering of driving rain, slightly supplemented by supercooling condensation. Brick 'B' shows higher variation in average moisture content due its lower moisture buffering capacity. During summer, brick 'A' buffers all driving rain during the time period shown while brick 'B' exhibits one event of runoff. The low average moisture content during no-rain periods is caused by intensive drying of the bricks during sunny and warm days.

Table 1 states the annual percentage of time (T) that runoff occurs and the total amount of runoff (Q) over one year for material A, for the different locations on the building types and for different orientations. We note that the height of the building or the presence of a gap/underpass slightly affect the runoff amounts at the top corners. These differences are caused by changes in the wind pattern at the top corner. The center of the buildings is entirely sheltered for driving rain, with exception of the building with gap. Simulations for other positions on building 'a' (southwest, brick 'A') (results not shown here) point out that runoff only occurs on the upper edge of the building. This is in accordance with the catch ratio distribution shown in Figure 5a. The largest part of the facade however never experiences runoff.

	T %	Q L/m²yr		T %	Q L/m²yr		T %	Q L/m²yr
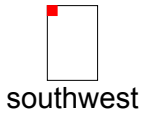 southwest	4.2	245	 southwest	0	0	 northeast	0.01	0.3
 southwest	3.4	201	 southwest	0	0	 southeast	0.6	44
 southwest	3.2	188	 southwest	0.6	23	 southwes t	4.2	245
 southwest	3.6	211	 southwest	0	0	 northwest	1.9	164

Table 1: Annual percentage of time (T) that runoff occurs and total amount of runoff (Q) over one year for material A, for different locations and for different orientations.

Figure 7 depicts the annual frequency distribution of runoff intensity for different places on the facade, different orientations and materials. The runoff generally has low intensity (< 2 l/m².h). Distributions are most extreme for the top corner. Lower runoff intensities are found beneath the gap. The center of the building is highly sheltered for high driving rain intensities and no runoff occurs. The northeast orientation receives less driving rain and consequently a lower occurrence of runoff is observed.

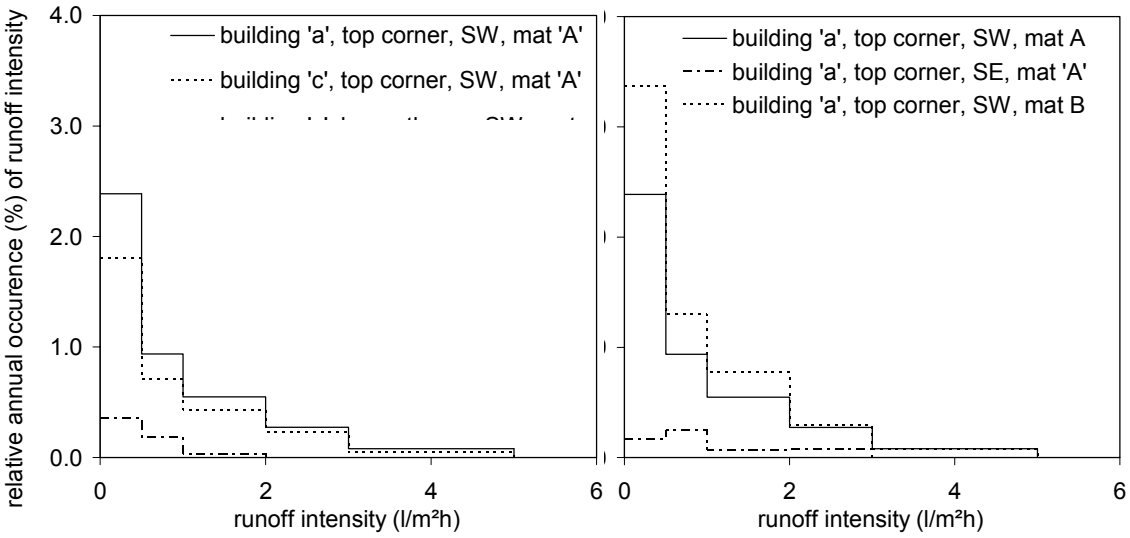

Figure 7: Annual frequency distributions of runoff intensity for different places on the facade, different orientations and different materials.

6 Runoff and the risk on rain penetration

For the ceramic bricks studied in this paper, it has been demonstrated that large parts of the facades have ample buffering capacity for all impinging driving rain. Rain penetration through the open vertical joints is therefore improbable, as no continuous water film over the open joints will arise. Moreover was it demonstrated that any occasionally occurring runoff takes place with low to very low intensities.

The behavior of water film flow at such low runoff intensity is investigated experimentally by means of film flow measurements, in which an artificial water film flow is imposed on a part of two layers of thin layer mortar brickwork (Figure 8). An evenly distributed water film is obtained by use of a saturated sand stone ridge for the overflowing top reservoir. The moisture flow is measured at 7 l/mh, which is relatively high.

For different materials and different initial states, it is noted that no continuous water film develops over the open vertical joints. Wind pressures, gravity or capillarity can thus not force water through the facade. Adhesion and the thin layer mortar geometry do result in a substantial drainage of the water film towards the open vertical joint though: the slightly set back horizontal mortar joint intercepts the water film, and channels all arriving water to the vertical joint. The geometry of the mortar strip and the geometry and roughness of the bricks will there dictate whether the water is drained back toward the exterior surface or penetrates to the inner surface of the outer leaf (Figure 8). Given the low intensity of the runoff, this is not problematic since the lower, less exposed and hence dryer parts of the brick façade have adequate buffering capacity left, and will easily absorb both interior and exterior runoff.

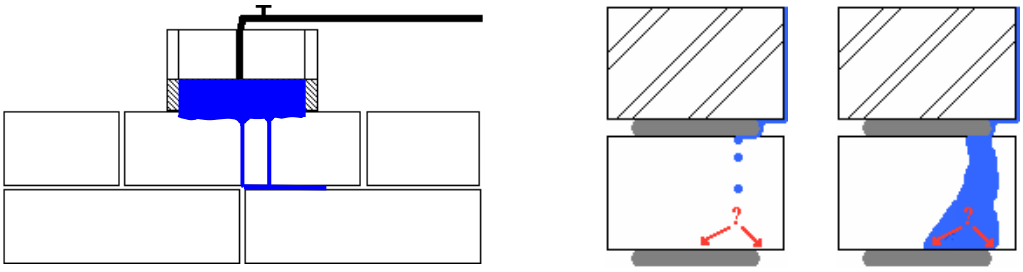

Figure 8: Experimental set-up for film flow measurements, front view (left) (fingering due to the initially dry state) and cross section view (right).

7 Conclusions

In this paper, the risk on rain penetration through open vertical joints in thin layer mortar ceramic brick facades has been scrutinized through combined CFD and HAM modeling. Direct impinging of rain drops is improbable, which makes the presence of a continuous water film over the open joints a premise for potential rain penetration. The results from driving rain and moisture transfer simulations did however indicate that large parts of the facades are relatively sheltered, and have sufficient buffering capacity to avoid runoff.

It was established that low intensity runoff occasionally occurs at the upper edges. From experiments it was concluded however that such runoffs do not yield a continuous water film over the open vertical joint, which leaves the premise for rain penetration due to wind pressure, gravity or capillary forces hence unfulfilled. The geometry of the brickwork and adhesive forces do however lead a substantial amount of the runoff to the vertical joints, where the geometry of the mortar strips, and the geometry and roughness of the bricks will determine their interior or exterior drainage. Low intensity interior runoff will easily be absorbed by lower, less exposed and thus

drier parts of the façade. The risk on severely penalized rain penetration through thin mortar layer brick facades with open vertical joints can therefore be considered low. This conclusion will however only hold for the ceramic brick as studied in this paper, as the lower absorption and buffering capacity of concrete brick will yield more frequent and more intense runoff, and thus potentially more severe rain penetration.

References

Best, A.C. 1950. The size distribution of raindrops. Quarterly Journal of the Royal Meteorological Society 76, 16-36

Blocken, B., Carmeliet, J. 2000a, Driving rain on building envelopes – I: numerical estimation and full-scale experimental verification, Journal of Thermal Envelope and Building Science 24, 61-85.

Blocken, B., Carmeliet, J. 2000b, Driving rain on building envelopes – II: representative experimental data for driving rain estimation. Journal of Thermal Envelope and Building Science 24, 89-110.

Blocken, B., Carmeliet, J. 2002, Spatial and temporal distribution of driving rain on a low-rise building. Wind and Structures 5, 441-462.

Blocken, B., H. Janssen and J. Carmeliet, 2002, On the modeling of runoff of driving rain on a capillary active surface, in proceedings of the "11th Symposium of Building Physics", 26-30 September 2002, Dresden, Germany, 400-408.

Carmeliet, J., Roels S., 2001, Determination of the isothermal moisture transport properties of Porous building Materials, Journal of Thermal Envelope and Building Science, 24, 183-210.

Carmeliet, J., Roels S. 2002, Determination of the moisture capacity of porous building materials, Journal of Thermal Envelope and Building Science 25, 209-237.

Celia, M.A., E.T. Bouloutas and R.L. Zarba, 1990, A general mass-conservative numerical solution for the unsaturated flow equation, Water Resources Research 26, 1483-1496.

Grunewald, J., 1997, Diffusiver und konvektiver stoff- und energietransport in kapillarporösen baustoffen, PhD-thesis, Technische Universität Dresden, Dresden, Germany.

Janssen, H., 2002, The influence of soil moisture transfer on building heat loss via the ground, Ph.D. thesis, Katholieke Universiteit Leuven, Belgium.

Künzel, H.M., 1993, Rain loads on building elements. Contribution to the IEA-Annex-24 meeting, Report T2-D-93/02, Holzkirchen, Germany.

Sneyers, R., E. Meert, D. Soubrier and G. Van Ackere, 1979, Intensité de la pluie battante et pression du vent sur les facades, C.S.T.C. revue 2.